Applied Meteorology Unit (AMU)

Quarterly Report

Fourth Quarter FY-00

Contract NAS10-96018

31 October 2000

ENSCO, Inc.
1980 N. Atlantic Ave., Suite 230
Cocoa Beach, FL 32931
(321) 853-8202 (AMU)
(321) 783-9735

SMC/SDEW/L. Hagerman
NOAA "W/NP"/L. Uccellini
NOAA/OAR/SSMC-I/J. Golden
NOAA/ARL/J. McQueen
NOAA Office of Military Affairs/L. Freeman
Aerospace Corp/T. Adang
NWS Melbourne/B. Hagemeyer
NWS Southern Region HQ/"W/SRH"/X. W. Proenza
NWS Southern Region HQ/"W/SR3"/D. Smith
NSSL/D. Forsyth
NWS/"W/OSD5"/B. Saffle
FSU Department of Meteorology/P. Ray
NCAR/J. Wilson
NCAR/Y. H. Kuo
30 WS/CC/P. Boerlage
30 SW/XP/J. Hetrick
NOAA/ERL/FSL/J. McGinley
ENSCO Contracts/E. Lambert

Executive Summary

This report summarizes the Applied Meteorology Unit (AMU) activities for the fourth quarter of Fiscal Year 00 (July – September 2000). A detailed project schedule is included in the Appendix.

Ms. Lambert continued work on the Statistical Short-Range Forecast Tools task with the goal of developing short-range ceiling forecast equations to be used in support of Shuttle landings. She continued an exploratory data analysis using a 20-year record of hourly surface observations (1978–1997) from stations in east-central Florid, centering on the ceiling thresholds defined by the Shuttle Flight Rules (FR). She calculated the 1- to 24-hour lag correlations between ceiling height observations at the Shuttle Landing Facility (SLF) and several other stations. Strong correlations exist for short lag times of 1 to 4 hours, but only weak correlations exist for longer time lags out to 24 hours. This eliminates the possibility that the observation 24 hours previous to the valid forecast time has predictive value in east-central Florida.

Mr. Wheeler and Dr. Short evaluated Core Aspect Ratio (CAR) data from the Weather Surveillance Radar model 88 Doppler (WSR-88D) and its possible use in predicting high wind and hail events. Rapid variations in CAR are often observed in convective cells that generate strong wind gusts and/or large hail. Using the model developed in Wheeler (1998), they found that replacing cell-based vertically integrated liquid (CVIL) with CAR produced a minor degradation in model skill. This is significant for the Interactive Radar Information System (IRIS) SIGMET Processor Evaluation task in which products will be developed using data from the Weather Surveillance Radar model 74C (WSR-74C) on Patrick Air Force Base. The CAR algorithm is much less complicated than the CVIL algorithm and would likely take less time to compute in IRIS. This would allow the model to be used with WSR-74C data as well as WSR-88D data.

Dr. Short continued Phase II of the IRIS SIGMET Processor Evaluation task. He is developing new radar products to meet the operational requirements of the 45th Weather Squadron (45 WS) and the Spaceflight Meteorology Group (SMG) using SIGMET Inc.'s IRIS system on the WSR-74C. Dr. Short developed an algorithm that generates a map of wind gust potential (WGP) as a function of vertically integrated liquid (VIL) and storm top information. He also developed an algorithm to compute the fractional coverage of radar echoes 18 dBZ or greater within 20 nm of the SLF to be used by SMG forecasters when evaluating FRs.

Mr. Wheeler completed the study on source regions of suspected chaff radar returns. Weather radar returns from chaff can mask meteorological signals, or at least complicate the job of interpreting meteorological returns for the 45 WS, SMG, and the National Weather Service in Melbourne, FL (NWS MLB). He determined that most of the 47 chaff releases documented during the data collection period occurred east of 85° west (W) longitude. Chaff events occurred during three launch attempts in the data collection period, and all three releases were east of 85° W longitude. Many of these events lasted over 10 hours.

Mr. Case continued the evaluation of the Regional Atmospheric Modeling System (RAMS) component of the Eastern Range Dispersion Assessment System (ERDAS). He compiled preliminary statistics to determine RAMS 1999-2000 cool season performance in forecasting frontal passages over Florida and low-level temperature inversions at Cape Canaveral Air Force Station (CCAFS), and calculated the gridded errors between the RAMS innermost grid and the Kennedy Space Center/CCAFS wind tower network. He also developed a technique to verify convection initiation in RAMS for the 2000 warm season.

Mr. Case continued work on Phase III of the Local Data Integration System (LDIS) task, which calls for AMU assistance to install a working LDIS at SMG and NWS MLB that generates routine high-resolution products for operational guidance. He was able to install the LDIS successfully at SMG, where it is now running in real-time. Due to hardware and software issues, the installation at NWS MLB has been delayed.

Mr. Dianic continued work on the Extension/Enhancement of the ERDAS RAMS Evaluation task to improve the archived database, and to perform sensitivity tests to identify the possible cause(s) of the model cold bias. He conducted a RAMS simulation using the Eta 0-h forecasts as the background field, and another simulation without the innermost fourth RAMS grid. Mr. Dianic began exploring the issues related to transferring point forecasts to NWS MLB and SMG, and installed software that is necessary to run RAMS on an AMU workstation.

Table of Contents

SPECIAL NOTICE TO READERS

AMU Quarterly Reports are now published on the Wide World Web (WWW). The Universal Resource Locator for the AMU Home Page is:

http://technology.ksc.nasa.gov/WWWaccess/AMU/home.html

The AMU Home Page can also be accessed via links from the NASA KSC Internal Home Page alphabetical index. The AMU link is "CCAS Applied Meteorology Unit".

If anyone on the current distribution would like to be removed and instead rely on the WWW for information regarding the AMU's progress and accomplishments, please respond to Frank Merceret (321-867-0818, francis.merceret-1@ksc.nasa.gov) or Winifred Lambert (321-853-8130, lambert.winifred@ensco.com).

1. BACKGROUND

The AMU has been in operation since September 1991. Tasking is reviewed annually with reviews at least semi-annually. The progress being made in each task is discussed in Section 2 with the primary AMU point of contact reflected on each task and/or subtask. A list of acronyms used in this report immediately follows Section 2.

2. AMU ACCOMPLISHMENTS DURING THE PAST QUARTER

2.1   TASK 003 SHORT-TERM FORECAST IMPROVEMENT

SUBTASK 3   STATISTICAL SHORT-RANGE FORECAST TOOLS (MS. LAMBERT)

The forecast cloud ceiling at the Shuttle Landing Facility (SLF) is a critical element in determining whether a GO or NO GO should be issued for a Space Shuttle landing. However, forecasters have found that ceiling is a difficult parameter to forecast. The goal of this task is to develop short-range ceiling forecast equations to be used in support of Shuttle landings. Ms. Lambert is using a 20-year record (1978–1997) of hourly surface observations from the SLF and several stations in east-central Florida to develop these equations. The equation development is centered on the ceiling thresholds defined by the Shuttle Flight Rules (FRs) as defined in Table 1.

Table 1. List of Flight Rules for ceiling thresholds at the Shuttle Landing Facility (SLF).	
Ceiling Threshold	**Flight Rule**
< 5000 ft	Return to Launch Site (RTLS)
< 8000 ft	End of Mission (EOM)
< 10 000 ft	Navigation Aid Degradation

During this quarter, Ms. Lambert continued the exploratory data analysis (EDA) of 20 years of hourly surface observations from the SLF (TTS) and several stations in east-central Florida. Those stations include

- Daytona Beach,

- Sanford,

- Orlando,

- Patrick Air Force Base,

- Melbourne, and

- Vero Beach.

Ceiling height values were separated into five categories:

- Category 1: ≤ 5000 ft
- Category 2: ≤ 8000 ft
- Category 3: $\leq 10\ 000$ ft
- Category 4: $\leq 15\ 000$ ft
- Category 5: $> 15\ 000$ ft

She then calculated the correlations between the category observations at the same time and at time lags from 1 to 24 hours. This was done in order to determine the predictive value of previous ceiling observations for the TTS ceiling observation at a specified valid time. It was also done to test a result found in Hilliker and Fritsch (1999) that the observation 24 hours previous to the forecast valid time is also a good predictor. Figure 1 shows a sample of the results in comparing TTS data only and TTS data with data from Patrick Air Force Base (COF, 3-letter identifier), the closest station.

24-Hour Cloud Ceiling Correlations
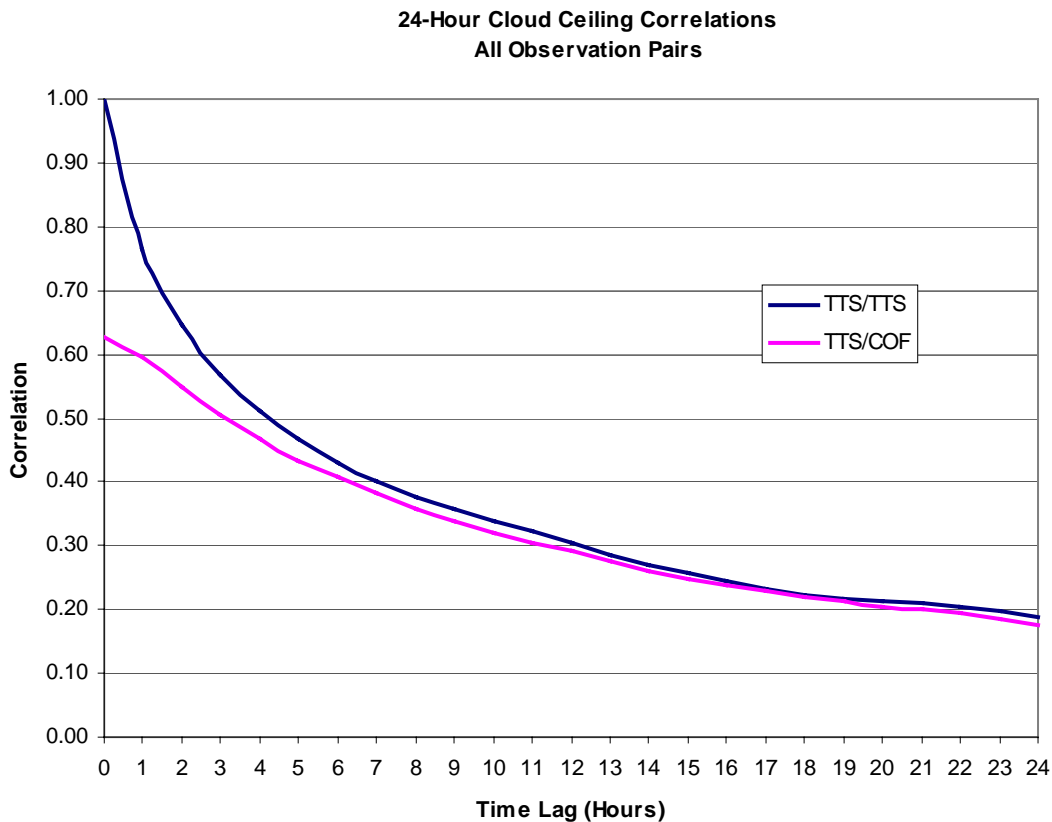**All Observation Pairs**

Figure 1.   Correlations between all ceiling category pairs observed over all hours of the day at time lags from 1 to 24 hours. The blue line shows the correlations between the categories at TTS alone, and the purple line shows the correlations between TTS and COF.

In Figure 1, the correlations of TTS data with itself are relatively high (> 0.5) for lag times up to 4 hours. It appears then, that these short lag time observations at TTS would be good ceiling category predictors. This is consistent with the findings of Vislocky and Fritsch (1997) and Hilliker and Fritsch (1999). The observations at COF also appear to have good predictive value, remaining above 0.5 for lag times up to 3 hours. The values decrease with increasing time lag, as would be expected. However, they do not increase as they approach 24 hours. This discards the possibility that the observation 24 hours previous to the valid forecast time has predictive value in east-central Florida. Although the values vary somewhat, the comparison with COF is representative of the other stations. In general, the larger the distance between TTS and the station, the lower the correlations in the shorter time lags.

After concluding the correlation tests, Ms. Lambert met with Drs. Manobianco and Short to discuss other appropriate predictors for cloud ceiling in east-central Florida. She separated the database into a development data set with which the equations will be developed and a testing data set on which the equations will be tested, and created predictors for input to forecast equation development routines.

References

Hilliker, J. L., and J. M. Fritsch, 1999: An observations-based statistical system for warm-season hourly probabilistic forecasts of low ceiling at the San Francisco International Airport. *J. Appl. Meteor.*, **38**, 1692-1705.

Vislocky, R. L., and J. M. Fritsch, 1997: An automated, observations-based system for short-term prediction of ceiling and visibility. *Wea. Forecasting*, **12**, 31-43.

2.2   TASK 004 INSTRUMENTATION AND MEASUREMENT

SUBTASK 5   I&M AND RSA SUPPORT (MR. CASE AND MR. WHEELER)

At the request of the 45th Weather Squadron (45 WS), Mr. Wheeler attended the Range Standardization and Automation (RSA) Weather Subsystem Screen Review presented by Raytheon Corporation in Denver, Colorado in September. Raytheon presented updated utilities and weather data displays and allowed attendees to review the displays and functionality. The 45 WS also requested that Mr. Wheeler and Mr. Case participate in an additional workshop at the Forecast Systems Laboratory (FSL) in Boulder, Colorado. The 30th Weather Squadron, 45 WS, and other RSA screen review participants also attended this workshop. FSL presented an overview of the architectural and timeline development of the Advanced Weather Interactive Processing System (AWIPS). In addition, FSL provided an overview of their recommended configuration for the Local Analysis and Prediction System (LAPS) and Regional Atmospheric Modeling System (RAMS) for RSA. Individual workgroup sessions discussed the LAPS/RAMS modeling effort, the capability of AWIPS to ingest and handle local datasets, and scripting language issues.

Table 2. AMU hours used in support of the I&M and RSA task in the fourth quarter of FY 2000 and total hours since July 1996.	
Quarterly Task Support (hours)	*Total Task Support (hours)*
52	301.5

SUBTASK 11   DETECTING CHAFF SOURCE REGIONS (MR. WHEELER)

The AMU was tasked to monitor, archive and analyze suspected chaff events with the primary goal of determining the source region for each event. Chaff is used by the military to mask aircraft and other operations. When dropped from an aircraft in the northeastern Gulf of Mexico on clear days with northwest flow aloft, chaff will generally drift with the wind and move across central Florida within hours. Chaff can mask meteorological echoes and make the interpretation of meteorological echoes difficult when they are mixed with chaff (Roeder 1995). This can have adverse effects on launch and landing operational forecasts at Kennedy Space Center (KSC) during rapidly changing weather conditions when weather launch commit criteria (LCC) and FRs are being evaluated. Chaff releases east of 85° (west) W longitude are suspected to be the source region of chaff radar returns over KSC during the winter months when strong west to northwest upper-level flow is prevalent. Current agreements restrict military chaff drops east of 85° W longitude during shuttle operations to protect launch and landings at KSC.

Chaff signatures were identified based on patterns and magnitude of reflectivity. Each chaff event in this study was identified and documented by using all available Weather Surveillance Radar 1988 Doppler (WSR-88D) level IV data from SIL (Slidell, LA), NPA (Pensacola, FL), TLH (Tallahassee, FL), TBW (Ruskin, FL), JAX (Jacksonville, FL) and MLB (Melbourne, FL) and the Weather Surveillance Radar model 74C (WSR-74C) SIGMET Integrated Radar Information System (IRIS) radar system. The WSR-88D Principle User Processor (PUP) in the AMU was used as the radar analysis tool. The WSR-74C radar data allowed for comparison of returns from the two radars following Merceret (1993). Visible satellite images and rawinsonde data from TBW, TLH, JAX, and Cape Canaveral Air Force Station (CCAFS, XMR – 3-letter identifier) were also saved for most days with chaff events to characterize the environmental moisture and winds.

Previous work (see Merceret 1993 for details) suggests the following criteria be used to determine whether a radar echo is caused by chaff:

1. Chaff moves with the mean wind.

2. Chaff shows a signature in the WSR-88D velocity field that is consistent with the wind field.

3. Chaff returns a stronger signal with the WSR-88D than the WSR-74C by approximately 17 dBZ because of the difference in radar wavelengths (10 cm vs. 5 cm, respectively).

4. Chaff is resonant at 10 cm and 5 cm wavelengths, but not at the 3 cm wavelength found in aircraft radars. This means that aircraft radars will not likely detect chaff.

5. Cross-sections and echo top products are needed to determine the height of the radar echo and to determine the fall-rate of the echo over time, which is approximately 3000 feet/hour for chaff.

6. Criteria 3 and 4 may not be valid for chaff that is cut to different wavelengths than 10 cm, but Criteria 1, 2, and 5 should still apply.

Only Criteria 1 and 3 were evaluated in this study. Criterion 2 was not evaluated because the mean wind field was determined strictly using rawinsonde data. Criterion 5 would have required an archive of WSR-88D level II data from several sites for post-analysis of radar cross-sections through the echoes as they evolved over time, and Criterion 6 would have required the acquisition and display of aircraft radar data. However, the customer requested that such an extensive evaluation of WSR-88D data not be done. Since the main objective of this task was to track chaff releases to their source region, it was deemed sufficient to determine a point of origin using radar data and to determine if the echo followed the mean wind using rawinsonde data.

Chaff Effects on Launch Operations

Figure 2 details the Eglin Air Force Base (AFB), FL warning areas with the number of scheduled exercises highlighted by color. Green shading depicts areas that have more than 10 000 scheduled exercises per year. They are mainly over the northeast (NE) Gulf of Mexico. If chaff resonant at 10 cm were released in these areas at high altitudes (above 20 000 ft) and with an expected fall velocity of about 3000 ft/hr, it would take hours for the chaff to reach the surface. Any chaff released by aircraft into these areas with a west to northwest upper-level wind flow would migrate with the wind into central Florida before reaching the surface.
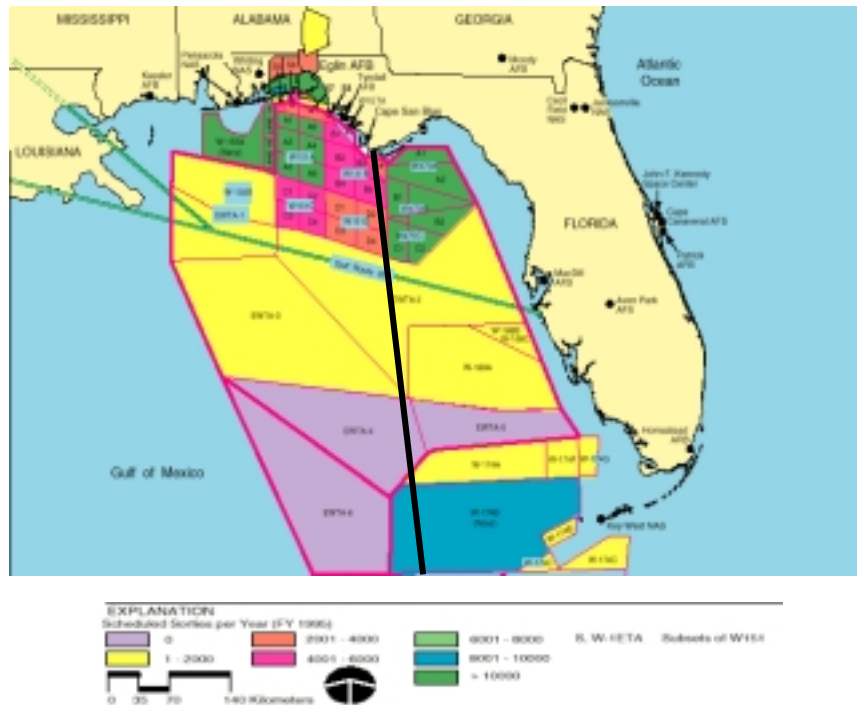
Figure 2.   Weapon system test ranges controlled by Eglin AFB, FL. Green shading (NE Gulf of Mexico) highlights areas that have more than 10 000 exercises per year. This entire area is east of 85° W longitude, indicated by the black line.

Numerous chaff events have been observed with the WSR-88D radars over Florida. In fact, chaff may cause the radar to switch from clear-air mode to precipitation mode in the absence of actual precipitation. In April 1993 during Shuttle Transportation System (STS-56) launch operations, a radar signature was noted on the National Weather Service in Melbourne, FL (NWS MLB) WSR-88D that seemed to be caused by anomalous propagation (AP). Satellite imagery indicated no apparent shower activity over central Florida at the time. The echoes detected by the WSR-88D created concern among the forecasters during the pre-launch operation.

Because of the concern and uncertainty about the phenomenon during STS-56 operations, the 45 WS requested AMU assistance in determining the cause of the WSR-88D signatures as a "mission immediate" task. Dr. Frank Merceret of the AMU reviewed and analyzed the data from both the WSR-88D and WSR-74C radars and determined that the echo was from needle chaff (Merceret 1993). Through his analysis of radar theory he determined that a difference of 17dBZ between the two radars could be expected when they are looking at the same 10 cm resonant needle chaff target. The reflectivity difference depends on the radar wavelengths and the length of chaff needles. With properly calibrated radars, the WSR-88D will have a stronger return from the same echo.

To help the Spaceflight Meteorology Group (SMG) evaluate weather FRs and the 45 WS evaluate LCCs, the Department of Defense (DOD) Eastern Area Frequency Coordinator (EAFC) issues what is called "Chaff De-confliction Messages" to preclude chaff drops that could affect Space Shuttle launches and landings and other launches at KSC/CCAFS. This de-confliction was intended to prevent the chaff echoes from interfering with real-time weather analysis of radar data.

Chaff Events

The occurrence of chaff signatures tends to increase during the cool season when well-organized convection associated with strong synoptic systems moves through the southeast United States (SE US). As these systems exit Florida, very dry air filters into the SE US, including Florida, setting the stage for several continuous days void of precipitation. Radar observations indicate that extensive chaff is released into the atmosphere during these extended dry spells. It is possible that the lack of an active weather pattern across the northeastern Gulf of Mexico and Florida increases the chance that chaff will be released from aircraft controlled by Eglin AFB in the Florida panhandle. The lack of showers is ideal for military exercises to be conducted without interruption. Unfortunately, the prevailing northwesterly wind flow dominant during these periods helps carry the streamers of chaff across Florida and into the KSC/CCAFS area. A significant decrease in chaff activity is noted from June through November. This decline in chaff releases may be directly related to the increase in convective activity in the northeastern Gulf of Mexico and Florida, which limits military training exercises. Also, with the weaker upper-level wind flow any chaff released during this period may not reach the central Florida area.

The AMU documented and archived radar data from suspected chaff drop occurrences in the northeastern Gulf of Mexico into western and central Florida, including the KSC/CCAFS area from January through April 2000. Radar signatures of chaff were monitored during the normal workweek, Monday through Friday. Base level or composite reflectivity scan data were retrieved from SIL, NPA, TLH, TBW, JAX and MLB WSR-88Ds for the chaff evaluation. These data sets were then archived into the AMU PUP's database. The WSR-74C radar was also used for comparison and archive purposes. This allowed for comparison of returns from the two radars using Merceret's (1993) rule to determine if a radar signature was caused by a chaff release.

During the period January through April 2000, a total of 47 chaff events were documented and analyzed. Three of the events occurred during launch operations. Most of these chaff events originated from the northeastern Gulf of Mexico region, but there were a few over the Atlantic Ocean, east of Jacksonville, FL. Hardcopy printouts were made of the WSR-88D and SIGMET IRIS radar images during each detected chaff event. Visible satellite images and rawinsonde data from TBW, TLH, JAX, and XMR were also saved for most days with chaff events. A log was kept detailing the events of each day.

April 2000 Chaff Event

A probable chaff event occurred on 26 April 2000, the day of a scheduled Shuttle launch operation (STS-101). Generally the SE US weather was dominated by a high-pressure system. Dry air was in place in the mid to high levels of the atmosphere. An old frontal boundary was observed south of Florida in an approximate east – west orientation through the Florida Straits. The TBW (Figure 3) rawinsonde data indicate a dry atmosphere above 10 000 ft with the winds above 10 000 ft from the northwest at 30 to 75 kt up to 30 000 ft.
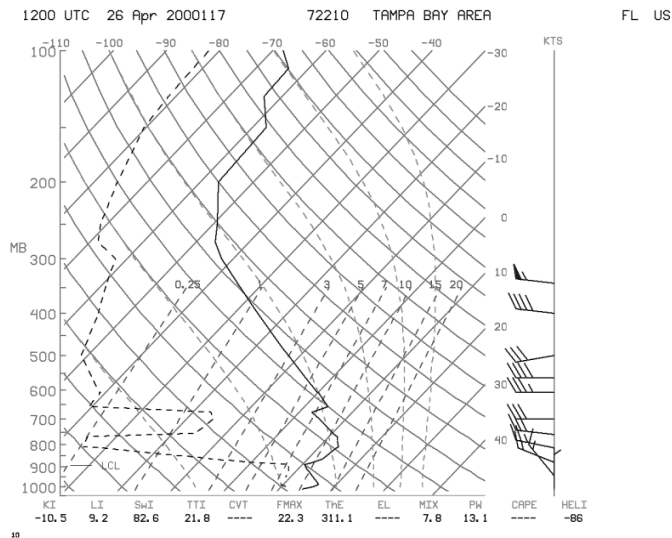
Figure 3.   Ruskin, FL (TBW) rawinsonde from 26 April 2000 at 1200 UTC indicates dry air above 900 mb.

The first indication of the suspected chaff release occurred at 1438 UTC (Figure 4). It appears that there were two chaff drop points: one in the northeast Gulf of Mexico, and the other southwest of TLH in the northern Gulf of Mexico. These signatures migrated east southeastward. The MLB WSR-88D image at 1531 UTC (Figure 5) shows a maximum return of greater than 28 dBZ southwest of Gainesville, FL (GNV). Figure 6 is a WSR-74C image showing a maximum return between 12 - 16 dBZ southwest of GNV at 1529 UTC. This 13 – 16 dBZ difference between the two radars is close to 17 dBZ identified by Merceret (1993) for chaff detection as described earlier. The ability to trace the radar signature back to a point of origin and the signature's tendency to move with the mean wind enhanced the probability that it was caused by chaff.
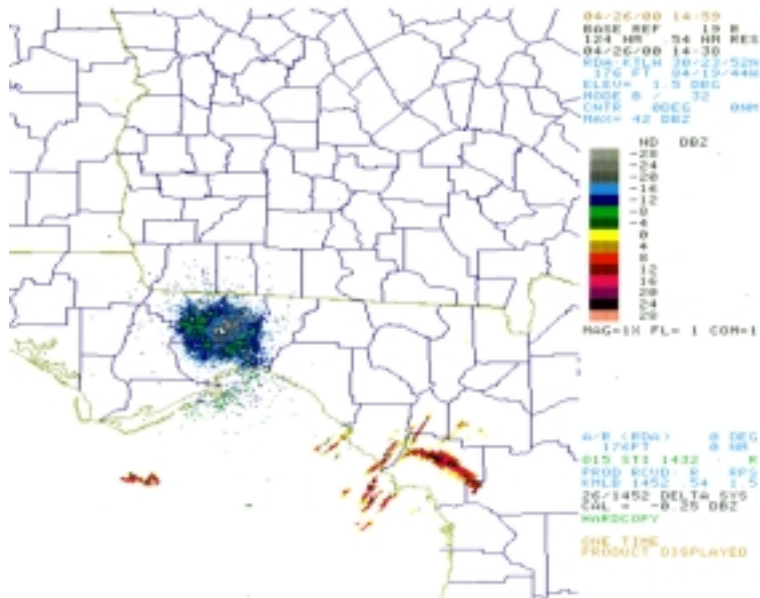
Figure 4.   TLH WSR-88D image from 26 April 2000 at 1438 UTC. Two chaff releases are indicated.
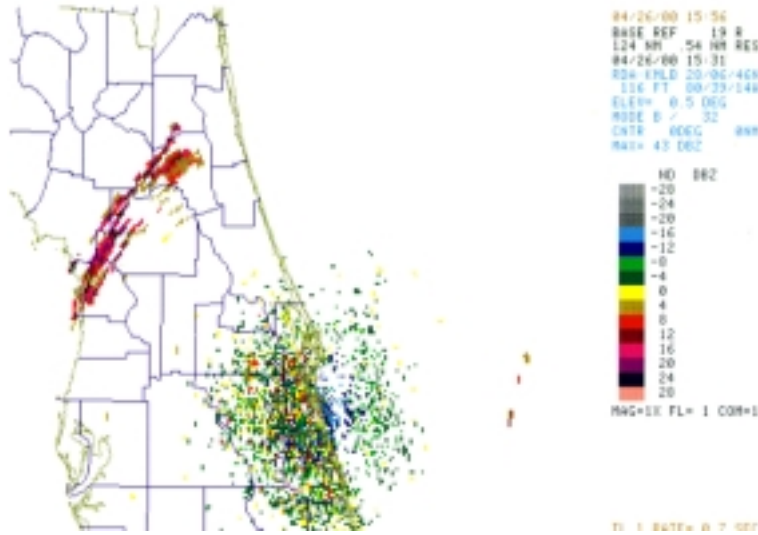
Figure 5.   MLB WSR-88D image from 26 April 2000 at 1531 UTC. Shows chaff signature of 25-30 dBZ, southwest of Gainesville, FL.

Figure 6.   PAFB WSR-74C image from 26 April 2000 at 1529 UTC. Shows 12-16 dBZ chaff return southwest of GNV.

   The chaff continued to migrate eastward and was over central Florida by 1650 UTC. Figure 7 shows the chaff signature moving over the KSC/CCAFS area by 1948 UTC, which is very close to the 1942 UTC opening of the launch window for STS-101. The extent of this chaff return during the launch window eliminated the SMG and 45 WS forecasters' capability to utilize the WSR-88D radar data for evaluating LCCs and FRs. The 45 WS was able to evaluate LCCs using WSR-74C data.
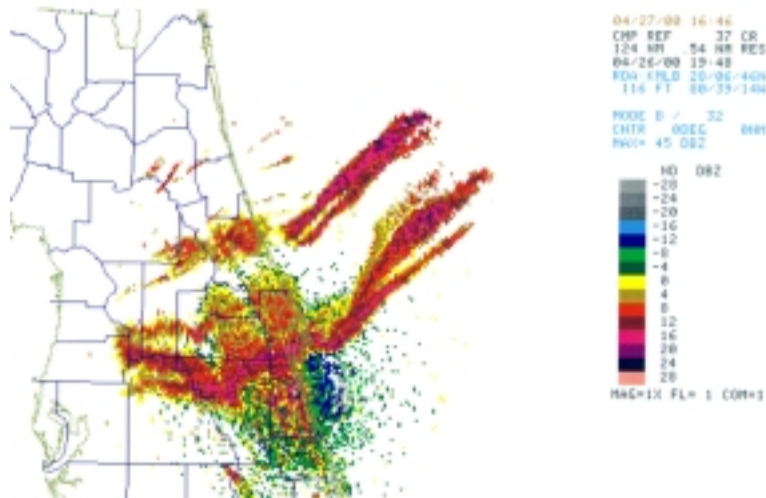
Figure 7.   MLB WSR-88D image from 26 April 2000 at 1948 UTC.   The chaff event has reached the KSC/CCAFS area.

Summary

The AMU monitored and archived suspected chaff events and determined the source region for each.   Current agreements restrict military chaff drops east of 85° W longitude during shuttle operations to protect launch and landings at KSC.   Chaff signatures were identified based on patterns and magnitude of reflectivity.   The AMU detected and tracked 47 probable chaff events during the period January through April 2000.   Three of the events occurred during launch operations.   Many of the 47 chaff events were released east of 85° W longitude and chaff was observed during 3 launch attempts in the data collection period with the releases east of 85° W.   Many of the events lasted for over 10 hours.

To help forecasters use radar data in evaluating LCCs and FRs, the DOD EAFC issues Chaff De-confliction Messages to preclude chaff drops that could affect launch and landing operations at KSC/CCAFS.   This message was intended to prevent the chaff echoes from interfering with real-time weather analysis of radar data.

For more information or a copy of the interim report, contact Mr. Mark Wheeler by phone at 321-853-8205 or by email at wheeler.mark@ensco.com.

References

Hullar, T. L., Fales, S. L., Hemond, H. F., Koutrakis, P., Schlesinger, W. H., Sobonya, R. R., Teal, J. M., Watson, J. G., 1999: Environmental Effects of RF Chaff. NRL/PU/6110-99-389, 81 pp.

United States General Accounting Office (GAO), 1998: DOD Management Issues Related to Chaff, GAO/NSIAD-98-219, 33 pp.

Roeder, W. P., 1995: Operational Impacts and Identification of Chaff on Weather Radar, 27th Conference on Radar Meteorology, 9-13 October 1995, 373-375.

Merceret, F. J., 1993: A Note on Needle Chaff as Viewed by Weather Radars, AMU Memorandum, 2 pp.

SUBTASK 12   SIGMET IRIS/OPEN PROCESSOR EVALUATION (DR. SHORT)

Phase II of the SIGMET IRIS Processor Evaluation task involves development of new radar products for meeting operational requirements of the 45 WS and SMG. IRIS provides display and analysis of radar reflectivity data from the WSR-74C located at Patrick Air Force Base (PAFB). Operational use of the radar and radar products includes evaluation of LCCs, FRs, and forecasting for ground operations.

Dr. Short developed prototype software that generates a map of wind gust potential (WGP) by using Vertically Integrated Liquid (VIL) and Storm Top (ST) information from the WSR-74C to evaluate a WGP equation. The equation, published by researchers at the WSR-88D Operational Support Facility (Stewart 1996), is:

$$WGP = [20.63 \times VIL - 3.125 \times ST^2]^{1/2},$$

where VIL is in mm and ST is in km.

This software automatically interrogates the radar product database, selects the appropriate VIL and ST files, computes WGP and inserts output into the IRIS database for display and analysis. The software was tested on an AMU workstation.

Dr. Short also developed prototype software that computes the percent of area within 20 nm of the SLF that is covered by rain. The software interrogates the IRIS product database, identifies the most recent product files and executes a secondary program. The secondary program accesses the most recent product of maximum reflectivity observed between 3000 ft and 60 000 ft out to 60 nm from the radar. It uses this product to compute the fractional coverage of echoes with reflectivities greater than 18 dBZ within 20 nm of the SLF. It also draws a circle of that radius around the SLF on the most recent image of this product and displays the percent coverage in a text box on the image.

References

Stewart, S. R., 1996: Wet microbursts - Predicting peak wind gusts associated with summertime pulse-type thunderstorms. Preprint volume for the 15th Conference on Weather Analysis and Forecasting, 19-23 August, Norfolk, Amer. Meteor. Soc., 324 - 327.

**SUBTASK 14   EXPLOIT NEXRAD: EXTENDED EVALUATION OF CORE ASPECT RATIO
(DR. SHORT AND MR. WHEELER)**

Rapid variations in Core Aspect Ratio (CAR) are often observed in convective cells that generate wind gusts greater than 35 knots and/or hail having a diameter of 0.50 inches or greater. The purpose of the task was to evaluate the potential predictive capabilities of CAR information with respect to wind gust and hail events for use in spacelift operations. Mr. Wheeler and Dr. Short performed the extended evaluation of CAR information that was generated during the Applied Meteorology Unit (AMU) Cell Trends study (Wheeler 1998).

The database used in the present study consisted of each cell's attributes of maximum reflectivity (MAX), height of the maximum reflectivity (HMAX), storm top (ST), cell-based vertically integrated liquid (CVIL) and CAR. The time resolution of a cell's trend, as determined by the WSR-88D volume scans, varied from 5 to 9 minutes. To create a homogeneous database for statistical modeling the time history of each of the 52 cells was interpolated to 0.5 minutes.

The analysis procedure was to identify all cells and track the trends in CAR, MAX, HMAX, ST and CVIL. A composite cell trend was obtained for wind gust and hail events by first defining an initial time (T_0) for each event. T_0 for each wind gust event was defined as the time at which simultaneous decreases in HMAX and CVIL were observed, according to the criteria established by Wheeler (1998) and those specified above. Similarly, T_0 for each hail event was defined as the time at which simultaneous increases in HMAX and CVIL were observed according to the criteria established by Wheeler (1998). The composite cell trends of MAX, HMAX, ST, CVIL and CAR for 15 wind gust events are shown in Figure 8a. The composite cell trends of MAX, HMAX, ST, CVIL and CAR for 6 hail events are shown in Figure 8b. Several of the hail events had time histories of only 10 minutes before T_0.
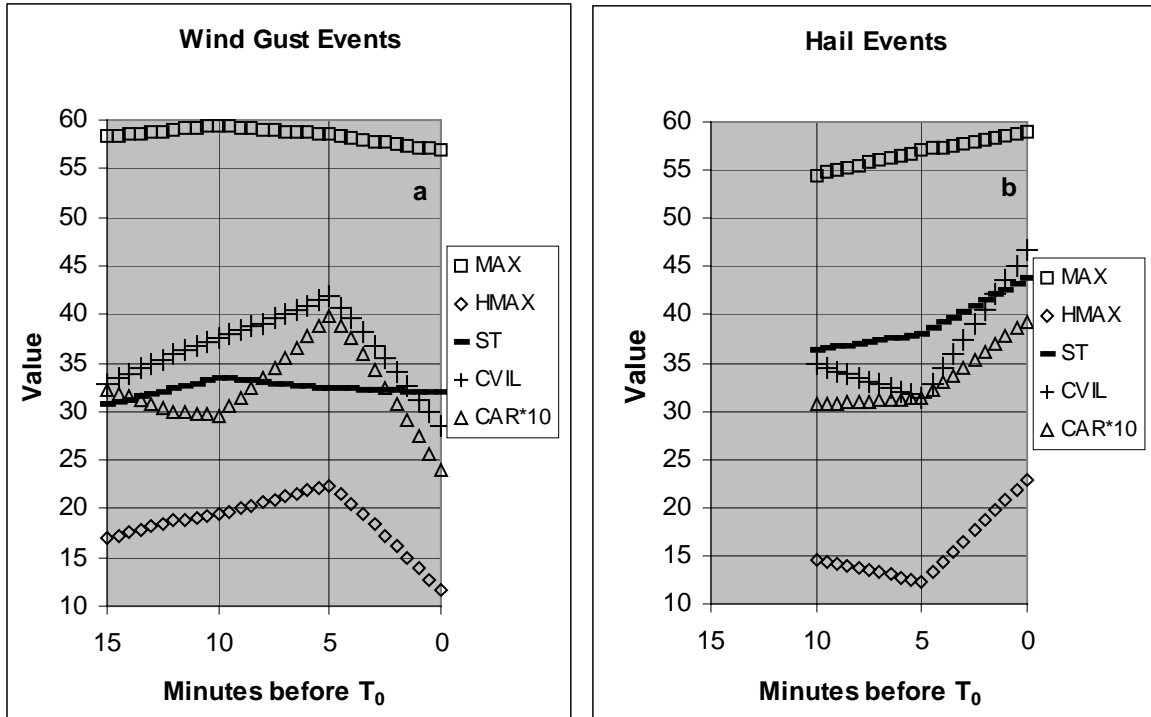
Figure 8.   Composite cell trends for a) Wind gust events and b) Hail events. Maximum reflectivity (MAX; dBZ), height of maximum reflectivity (HMAX; kilo-feet), storm top (ST; kilo-feet), cell-based vertically integrated liquid (CVIL; mm) and core aspect ratio (CAR; x 10) are shown.

Figure 8a shows that the average trends of HMAX, CVIL and CAR are sharply downward prior to wind gust events. Weak downward trends are also observed in the average MAX and ST parameters. These signatures are all consistent with a descending mass of hydrometeors, the causative mechanism of downbursts (Fujita 1985). Figure 8b shows that the average trends of HMAX, CVIL and CAR are upward prior to hail events. Upward trends are also observed in the average MAX and ST parameters. These signatures are all consistent with the presence of a strong updraft, required for the growth of hail.

Given the consistent signatures of HMAX, CVIL and CAR shown in Figures 2a and 2b, it seems reasonable to examine the value of CAR information for improving predictions of wind gust and hail events. The database used in Wheeler (1998) was re-examined to determine the predictive potential of CAR information when combined with CVIL and HMAX information. The basic structure of the original algorithm, shown in Figure 9, was adopted and tested using four standard measures of skill: False Alarm Rate (FAR), Probability of Detection (POD), Critical Skill Index (CSI), and Heidke Skill Score (HSS). Table 3 gives definitions of these measures in terms of the number of successful and unsuccessful forecasts.

Has HMAX decreased or increased by 8000 ft or more since the last observation?

Yes → Decreased   **No** → Stop   **Yes** → Increased

Is HMAX now 10 000 ft or higher?

Yes   **No** → Stop

Is HMAX now 18 000 ft or higher?

No → Stop   **Yes**

Has CVIL decreased by 10 mm or more since the last observation?

Yes   **No** → Stop

Has CVIL increased by 10 mm or more since the last observation?

No → Stop   **Yes**

Forecast wind gust > 35 knots

Forecast Hail ≥ 0.50 inches

Figure 9. A decision tree for forecasting wind gust and hail events, based on cell trends of HMAX and CVIL (Wheeler 1998).

Table 3. A four-cell contingency table used for the verification statistics.

		Observed Event	
		Yes	**No**
Forecast Event	**Yes**	a	b
	No	c	d

$N = a + b + c + d$

False Alarm Rate (FAR) $= b/(a+b)$

Probability of Detection (POD) $= a/(a+c)$

Critical Success Index (CSI) $= a/(a+b+c)$

Heidke Skill Score (HSS) $= [(a+d) - E]/(N-E)$

$E = [(a+c)(a+b)+(b+d)(c+d)]/N$

The approach used in testing the value of CAR information was to combine it with HMAX and CVIL, the successful predictors identified by Wheeler (1998). The decision tree shown in Figure 9 was used for the algorithm and modifications described below were made to test the impact of CAR information. However, in an effort to restrict the algorithm to three or four pieces of information, CAR was used to replace first one and then the other proven predictor.

Table 4 shows performance characteristics of various combinations of HMAX, CVIL and CAR cell trends when used to predict wind gust events. The original algorithm of Wheeler (1998) has excellent performance, as evidenced in the FAR, POD, CSI and HSS values. The combination of HMAX and CAR information was used by substituting CAR for CVIL in Figure 9 and requiring that the trend in CAR was negative. When CAR information was combined with HMAX, the FAR improved slightly, but the POD decreased slightly. Given the relatively small sample size and excellent performance of the Wheeler (1998) algorithm, it may be difficult to determine if the changes in performance increased statistically through sampling variations, or if they indicate an improved physical characterization of the event-producing cells. Nevertheless, this objective test does indicate that CAR information has predictive value when used in combination with HMAX.

The combination of CVIL and CAR was used by substituting CAR for HMAX in Figure 9, requiring that the trend of CAR was negative with an initial value > 3.0, and requiring that the initial CVIL value was > 30. When CAR was used in combination with CVIL the performance measures all decreased, relative to the original algorithm.

Table 4. Comparison of cell trends attribute statistics for microbursts.					
Microburst Signature (original algorithm; HMAX & CVIL)					
		Observed		FAR:	0.12
		Yes	No	POD:	0.94
Forecast	Yes	**15**	**2**	CSI:	0.83
	No	**1**	**35**	HSS:	0.86
Microburst Signature (HMAX & CAR)					
		Observed		FAR:	0.07
		Yes	No	POD:	0.87
Forecast	Yes	**14**	**1**	CSI:	0.82
	No	**2**	**36**	HSS:	0.87
Microburst Signature (CVIL & CAR)					
		Observed		FAR:	0.39
		Yes	No	POD:	0.87
Forecast	Yes	**14**	**9**	CSI:	0.56
	No	**2**	**28**	HSS:	0.56

Table 5 shows the performance characteristics of various combinations of HMAX, CVIL and CAR cell trends when used to predict hail events. The original algorithm of Wheeler (1998) had good performance, as evidenced in the skill scores. The combination of HMAX and CAR was used by substituting CAR for CVIL in Figure 9, requiring that the trend in CAR was negative and requiring that its initial value was > 3.0. When CAR information was combined with HMAX, the FAR decreased, but the POD also decreased. Because of the small sample size it is not known if this degradation is statistically significant.

The combination of CVIL and CAR was used by substituting CAR for HMAX in Figure 9 and by requiring that the trend in CAR be negative. When CAR was used in combination with CVIL the performance measures all decreased, relative to the original algorithm. These results are similar to what is shown in Table 4. Further analyses, detailed in a memorandum, have shown that changes in CVIL and CAR are weakly correlated, whereas HMAX and CAR are almost independent. The combination that is least correlated provided superior skill.

Table 5. Comparison of cell trends attribute statistics for hail.				
Hail Signature (original algorithm; HMAX & CVIL)				
	Observed		FAR:	0.40
	Yes	No	POD:	1.00
Forecast Yes	6	4	CSI:	0.60
No	0	43	HSS:	0.71
Hail Signature (HMAX & CAR)				
	Observed		FAR:	0.20
	Yes	No	POD:	0.67
Forecast Yes	4	1	CSI:	0.57
No	2	46	HSS	0.70
Hail Signature (CVIL & CAR)				
	Observed		FAR:	0.55
	Yes	No	POD:	0.67
Forecast Yes	4	5	CSI:	0.36
No	2	42	HSS:	0.46

The results of this study suggest that CAR information can be combined with HMAX information to predict wind gust and hail events with only a minor degradation of skill as compared to the combination of CVIL and HMAX information reported by Wheeler (1998). This may be important for the WSR-74C exploitation task because of the potentially high computational cost of producing a CVIL product on the SIGMET IRIS. A CVIL product requires determination of the vertical tilt of a cell at a number of closely spaced vertical levels. CAR may take less processing time to compute than CVIL because IRIS already has an ST product, a cell-tracking product and a MAX product. These can be used locate a cell, assign a maximum reflectivity, assign the height of its top, and determine the height of the maximum reflectivity by an intelligent search of the reflectivity database.

For more information or a copy of the memorandum, contact Dr. Dave Short by phone at 321-853-8105 or by email at short.david@ensco.com.

References

Wheeler, M., 1998: WSR-88D Cell Trends Final Report. NASA Contractor Rep. CR-207-904, 36 pp.

Fujita, T. T., 1985: The downburst: Microburst and Macroburst. SMRP Res. Paper No. 210 (NTIS PB 85-148880), 122 pp.

2.3 TASK 005 MESOSCALE MODELING

SUBTASK 4   DELTA EXPLOSION ANALYSIS (MR. EVANS)

The Delta Explosion Analysis project was funded by KSC under AMU option hours. The primary goal of this task was to conduct a case study of the explosion plume using the RAMS, Rocket Exhaust Effluent Dispersion Model (REEDM), and Hybrid Particle and Concentration Transport (HYPACT) model and compare the model results with available meteorological and plume observations. There were two reasons for the modeling exercise of comparing the observed and predicted plumes. The principal of the two reasons was to determine how well the modeled plume trajectories compared with the observed plume trajectories. The secondary reason was to determine how the REEDM-predicted source term compared with the actual source term. Mr. Evans completed revisions and distributed the final report in September.

SUBTASK 8   MESO-MODEL EVALUATION (MR. CASE)

The Eastern Range Dispersion Assessment System (ERDAS) is designed to provide emergency response guidance to the 45th Range Safety (45 SW/SE) in support of operations at the Eastern Range in the event of an accidental hazardous material release or an aborted vehicle launch. ERDAS uses the RAMS Numerical Weather Prediction (NWP) model to generate prognostic wind and temperature fields for input into ERDAS diffusion algorithms. In addition, RAMS predicts a number of other meteorological quantities on four nested grids with horizontal resolutions of 60, 15, 5, and 1.25 km, respectively. The 1.25-km grid is centered over KSC/CCAFS. Therefore, real-time RAMS forecasts provide an opportunity for improved weather forecasting in support of space operations through high-resolution NWP over the complex land-water interfaces of KSC/CCAFS. The 45 SW/SE and the 45 WS have tasked the AMU to evaluate the accuracy of RAMS for all seasons and under various weather regimes during 1999 and 2000.

This section summarizes the work performed this past quarter by the AMU in support of the ERDAS RAMS evaluation. The interim report on the 1999 warm-season evaluation of RAMS was distributed this past quarter. Mr. Case presented a paper titled "A sensitivity and benchmark study of RAMS in the Eastern Range Dispersion Assessment System" at the American Meteorological Society's 9th Conference on Aviation, Range, and Aerospace Meteorology in Orlando, FL. The presentation contained a small portion of the objective evaluation from the AMU interim report. The following sections contain descriptions of the methodology and some preliminary results of the 1999-2000 cool-season evaluation, a discussion of the modified sea-breeze evaluation for the 1999 and 2000 warm seasons, and the convective initiation verification technique for the 2000 warm-season.

1999-2000 Cool-season evaluation

Much of the work during the past quarter was spent developing the methodology and techniques for the 1999-2000 cool-season subjective evaluation of RAMS, which was conducted for the months of November 1999 to March 2000. Mr. Case developed evaluation techniques and compiled preliminary statistics for most of the required components of the 1999-2000 cool-season evaluation. These techniques include the following:

- Verification of frontal passages across the Florida peninsula.

- Verification of low-level temperature inversions at the CCAFS rawinsonde site (XMR).

- Gridded error statistics between RAMS grid 4 and gridded analyses of KSC/CCAFS wind tower data.

- Subjective precipitation evaluation, especially associated with frontal passages.

- Verification of nighttime low temperatures at the KSC/CCAFS wind towers.

The first three techniques are explained in more detail in the following sub-sections.

Verification of frontal passages

During the five cool-season months, Mr. Case documented all occurrences of any type of observed frontal discontinuities (wind shifts, temperature, or dew point temperature gradients). Graphical traces (meteograms) of hourly temperature, dew point temperature, and wind direction and speed observations and RAMS point forecasts were examined at seven selected surface stations in the Florida peninsula (Jacksonville, Daytona Beach, the SLF, Melbourne, Vero Beach, West Palm Beach, and Miami). Frontal passages were verified for both the 0000 UTC and 1200 UTC RAMS forecast cycles whenever the 24-h forecast overlapped an observed frontal passage. The discontinuities in winds, temperature, and dew point temperature were each verified independently because the wind shifts and temperature/dew point temperature gradients often occurred at different times with a frontal passage. The intensity of the frontal passage was verified by comparing the observed and forecast 3-h changes in each meteorological quantity following the initial discontinuity.

15

The results of this frontal verification indicate that RAMS has a tendency to under-represent the intensity of frontal zones, particularly with respect to moisture changes (see Table 6). RAMS has a bias of -4.6°C in the 3-h change in dew point temperature following a frontal passage, which means that the model is typically too weak in the moisture gradients associated with frontal passages over the Florida peninsula. RAMS also has a negative bias in the 3-h temperature change following a front (-1.9°C); however, much of this bias can be attributed to the prevailing cool bias in the model that typically precedes frontal passages (-1.6°C, 2nd row in Table 6). The root mean square (RMS) error in frontal timing is on the order of 2–4 h, with the model having a slight tendency to be slow in the advancement of the front, particularly with the wind shift line (2.2 h bias). A positive bias in frontal timing indicates that the time of the forecast frontal passage is typically later than the observed passage.

Table 6. A summary of the cold frontal verification at seven selected surface stations along the east coast of Florida (Jacksonville, Daytona Beach, SLF, Melbourne, Vero Beach, West Palm Beach, and Miami).

Category	Variable	RMS Error	Bias
Pre-frontal Errors	Wind Dirn. (deg)	36.2	-11.8
	T (°C)	3.0	-1.6
	T_d (°C)	2.6	1.1
Timing Errors	Wind shift (hours)	3.7	2.2
	T-change (hours)	2.2	0.2
	T_d-change (hours)	3.1	1.2
Frontal Errors	Δ Wind Dirn. (deg)	46.9	1.9
	Δ T (°C)	3.1	-1.9
	Δ T_d (°C)	6.1	-4.6
Post-frontal Errors	Peak Wind Speed (m s^{-1})	3.2	-2.5

Verification of low-level temperature inversions

For all five cool-season months, Mr. Case examined the occurrence of observed and forecast temperature inversions at XMR in the lowest 3 km of the atmosphere, including both surface-based radiation inversions and elevated subsidence inversions. Approximately 80% of the cases examined were surface-based radiation inversions. Both the 0000 UTC and 1200 UTC RAMS forecast cycles were examined and verified against the observed morning XMR sounding, which was typically released at about 1100 UTC. Therefore, the 11-h forecast from the 0000 UTC RAMS cycle and the 23-h forecast from the previous day's 1200 UTC RAMS cycle are the verifying forecast hours.

The number of model forecast "hits" and "misses" were compiled to determine how well RAMS can predict the occurrence of a temperature inversion. When both an observed and forecast inversion occurred, specific parameters were verified including the intensity of the temperature inversion in °C, the height of the inversion base in meters, and the depth of the inversion in meters.

Tables 7 and 8 summarize the results of the temperature inversion verification. The 0000 UTC and 1200 UTC statistics are combined since the 0000 UTC RAMS cycle performed only marginally better than the 1200 UTC cycle (not shown). According to the contingency table in Table 7, RAMS has a tendency to under-predict the occurrence of low-level temperature inversions at XMR during the early morning hours. Although it has a very low FAR (0.03), RAMS also has a low POD (0.46) indicating that the model can predict only about 1 in every 2 low-level inversions at XMR (Table 7).

Table 7. A contingency table of the number of RAMS forecast versus observed occurrences of low-level temperature inversions at the CCAFS rawinsonde during the period of November 1999 to March 2000.

		Observed	
		Yes	No
Forecast	Yes	**86**	**3**
	No	**103**	**15**

Probability of Detection: 0.46
False Alarm Rate: 0.03
Bias: 0.47

When RAMS successfully forecasts a low-level inversion, the model typically underestimates the intensity of the inversion by 2.5°C (bias of -2.5°C in Table 8). The RMS errors in forecast inversion depth and height of the inversion base are 202 m and 516 m, respectively. The model has a slight tendency to spread the inversion through a deeper layer than observed (59 m bias). Not directly indicated in these tables is the difficulty that RAMS demonstrated in its ability to consistently predict surface-based inversions. Many surface-based inversions were either not forecast by RAMS, or the predicted inversion occurred above the surface in the lowest 1 km.

Table 8. A summary of the root mean square (RMS) error and bias statistics of the RAMS forecast temperature inversion intensity (°C), depth of the inversion (m), and height of the inversion base (m), using the CCAFS rawinsonde from November 1999 to March 2000.

Parameter	RMS Error	Bias
Intensity (°C)	4.1	-2.5
Depth (m)	202	59
Height (m)	516	22

Gridded error statistics on RAMS grid 4

One portion of the ERDAS RAMS evaluation is to compute gridded error statistics between objectively analyzed KSC/CCAFS wind-tower observations and RAMS grid-4 forecast temperatures and winds. The goal of this exercise is to determine the spatial variability (if any) in the RAMS grid-4 forecast errors within the area of the KSC/CCAFS wind towers. The gridded analyses of KSC/CCAFS wind tower observations were generated using a Barnes (1964) objective analysis program available in the General Meteorological Package software. A program was written to extract forecast and objectively analyzed grids of 6-ft temperatures and 54-ft wind observations on the RAMS grid-4, and then calculate the bias and RMS error of forecast 6-ft temperatures and 54-ft winds. These errors were calculated for both RAMS initialization times of 0000 and 1200 UTC. The errors will be examined for the 1999-2000 cool season and the 2000 warm season in three ways listed below.

- The gridded error statistics will be computed at each available grid point for a specified range of forecasts (monthly or seasonal). The spatial errors will then be examined as a function of forecast hour.

- The area-averaged gridded errors will be computed for each individual forecast as a function of forecast hour.

- The area-averaged gridded errors will be computed over a specified range of forecasts (for example, an entire season) and examined as a function of forecast hour.

Preliminary results indicate that the cool temperature bias is a domain-wide phenomenon on grid-4, but shows some variability between the land and water. However, the cool bias over the water cannot be adequately determined because the KSC/CCAFS wind towers used in the objective analyses are located only over the land. The RAMS model generates a contrast between forecast temperatures over land versus water, with cooler air temperatures over water on average. Therefore, the spatial variability in temperature errors on grid-4 is merely a figment of the land-sea contrast in the model, which cannot be resolved by the wind-tower network. The wind field verification between the analyses and forecasts presents the same problem over the water regions. The RAMS forecast wind speeds are higher over water because of the reduced frictional drag in the model, whereas the objectively analyzed wind speeds are valid only over land. These findings illustrate the difficulty in verifying a high-resolution forecast model such as ERDAS RAMS. The model verification can only be as robust as the observational network used as ground truth.

Warm-season subjective evaluation

Two components of the warm-season subjective evaluation include a sea-breeze verification at selected KSC/CCAFS wind towers and a "first thunderstorm of the day", or convective initiation verification on the RAMS grid-4. The sea-breeze verification technique used for the 1999 warm season evaluation has been modified slightly to increase the sample size and improve the robustness of the verification. From the archived point forecasts at the KSC/CCAFS wind towers, the sea-breeze verification will be back-filled for days in 1999 when the real-time evaluation could not be conducted (such as non-working days and employee absences). In addition, the forecast sea-breeze occurrence will be verified on a per-tower basis at 12 selected towers, rather than identified anywhere in the wind-tower network. The forecast timing errors of the sea-breeze onset will also be examined at each of the 12 selected wind towers for all possible RAMS forecasts.

Finally, a technique was developed to verify convective initiation on the RAMS grid-4 for the 2000 warm season. The day's first observed thunderstorm is determined based on the first strokes detected by the Cloud to Ground Lightning Surveillance System (CGLSS) between 1500 and 2300 UTC. The first RAMS-predicted "thunderstorm" is identified based upon a set of empirical rules that realistically represent a model storm likely to be electrified. The results of the sea breeze and convective initiation studies will be presented in the upcoming RAMS final report in early 2001.

For more information or a copy of the interim report, contact Mr. Jonathan Case by phone at 321-853-8264 or by email at case.jonathan@ensco.com.

Reference

Barnes, S. L., 1964: A technique for maximizing details in numerical weather map analysis. *J. Appl. Meteor.*, **3**, 396-409.

SUBTASK 10   LOCAL DATA INTEGRATION SYSTEM PHASE III (MR. CASE)

The Local Data Integration System (LDIS) task emerged out of the need to simplify the generation of short-term weather forecasts in support of launch, landing, and ground operations. The complexity of creating short-term forecasts has increased due to the variety and disparate characteristics of the multitude of available weather observations. Therefore, the goal of the LDIS task is to generate high-resolution weather analysis products that may enhance the operational forecasters' understanding of the current state of the atmosphere, resulting in improved short-term forecasts. In Phase I, the AMU configured a prototype LDIS for east-central Florida that integrated all available weather observations into gridded analyses. In Phase II, the AMU simulated a real-time LDIS configuration using two weeks of archived data. The LDIS Phase III task calls for AMU assistance to the SMG and the NWS MLB to install a working real-time LDIS that routinely generates high-resolution products for operational guidance.

SMG Installation

During this past quarter, Mr. Case traveled to SMG and installed LDIS on their 2-processor Hewlett Packard (HP) workstation. Mr. Case coordinated with Mr. Oram and Mr. Garner of SMG to set up the most critical real-time data ingestors, including Rapid Update Cycle (RUC) model background grids, Geostationary Operational Environmental Satellite (GOES)-8 infrared and visible data, level III WSR-88D reflectivity and radial velocity data from four Florida radar sites (Melbourne, Tampa Bay, Miami, and Jacksonville), KSC/CCAFS wind tower and 50-MHz profiler data, and surface land, buoy, and ship observations. Mr. Case continued occasional remote assistance after the installation process in order to correct some minor problems. To date, the LDIS continues to run in real-time at SMG, generating analysis products on two grids with horizontal resolutions of 10 km and 2 km, respectively.

NWS MLB Installation

The installation of LDIS at the NWS MLB has been delayed for three reasons. First, a security issue must be resolved with Computer Sciences Raytheon (CSR) in order to access text data sets from the Meteorological Interactive Data Display System (MIDDS). The AMU, NWS MLB, and CSR have collaborated and determined a solution for obtaining the MIDDS data in real-time. This solution involves a direct-dial connection from the NWS MLB workstation to a CSR server that has posted the required data files. The AMU and CSR are currently working on additional details such as file formats. Once these details are finalized, the NWS MLB will be able to obtain the necessary MIDDS text files every 15 minutes for ingestion into LDIS.

A second issue that has affected the delivery is the preparation of level II WSR-88D data for ingest. In order to create data files in the format necessary for ingestion, the Radar Interface and Data Distribution System (RIDDS) software needs to be installed onto the HP workstation used for running LDIS at the NWS MLB. This software is maintained at the National Severe Storms Laboratory (NSSL) in Norman, OK, but only for a Sun hardware platform. Thus, technical collaboration is required between the AMU, NWS MLB, and NSSL to build the software on an HP platform. In addition, the RIDDS software requires a dedicated network connection to the RIDDS server at the NWS MLB. A few additional issues still remain, but the AMU and NWS MLB have made considerable progress in preparing this software for the LDIS HP workstation.

The third issue impacting the installation of LDIS at the NWS MLB involves hardware and software issues. In particular, the NWS MLB needs to purchase and install a licensed HP C-language compiler for their LDIS workstation. This compiler is required in order to maintain the LDIS software on their HP workstation. In addition, a second network card connected to the RIDDS server is required for a dedicated WSR-88D data feed to the HP workstation. The NWS MLB purchased both these items and already installed the network card. They are still waiting for the delivery of the C compiler from HP. Once these three issues discussed above have been resolved and further AMU testing is performed onsite, the NWS MLB should have the LDIS running in real-time using the high-resolution level II WSR-88D data from the Melbourne radar site, in addition to the MIDDS data sets described above.

**SUBTASK 11   EXTENSION / ENHANCEMENT OF THE ERDAS RAMS EVALUATION
                (MR. CASE AND MR. DIANIC)**

The Extension / Enhancement of the ERDAS RAMS Evaluation is being funded by KSC under AMU option hours. During the course of the evaluation under Subtask 8, the AMU discovered a systematic low-level cold bias in the RAMS forecasts. In addition, several RAMS forecasts were not successfully run in real-time due to various technical issues. As a result, KSC tasked the AMU to re-run historical RAMS forecasts to improve the archived data base, and to perform sensitivity tests to identify the possible cause(s) for the model cold bias. Also, depending on the remaining funds in the options hours task, the AMU will explore the possibility of transferring real-time RAMS forecasts to the NWS MLB and SMG offices, and to improve the ENSCO-generated graphical user interface that verifies RAMS forecasts in real time.

During the past quarter, the AMU tended to three items within the scope of the extension task. First, Mr. Dianic managed the execution of two types of sensitivity experiments. The first experiment involved re-running the 24-h forecasts of the full 4-grid configuration of RAMS using Eta 0-h rather than 12-h forecasts as background fields for the RAMS initial condition. Once enough forecasts have been collected for a statistically significant data set, the point error statistics from these experimental model runs will be compiled and compared to the original RAMS forecasts using Eta 12-h forecasts as background fields. The results from this comparison will be presented in the ERDAS RAMS final report in early 2001. The second sensitivity experiment managed by Mr. Dianic was the 3-grid simulation, in which RAMS was run without the innermost fourth grid to determine the impact of a reduction in horizontal resolution on model errors. The finest horizontal resolution of the 3-grid forecasts is 5 km compared to 1.25 km, the resolution of the RAMS grid 4.

Another task item is to examine the feasibility of transferring RAMS point forecasts and selected forecast grids to both the NWS MLB and SMG offices. If such a data transfer mechanism is possible, then the AMU will set up the transfer to each office such that forecasters can examine high-resolution RAMS forecasts over east-central Florida. In order to assess the feasibility of such a data transfer, two items need to be addressed. First, the utility of high-resolution RAMS forecasts may be somewhat limited if a minimum required data set cannot be transferred to each office. The AMU will determine the minimum amount of RAMS data necessary to provide added value at each forecast office. Second, the AMU will determine if a transfer mechanism can meet this minimum requirement, given the available communications bandwidth. Mr. Dianic began exploring these issues regarding a possible data transfer mechanism.

Finally, the Message Passing Interface (MPI) software was installed onto the AMU 4-processor HP workstation this past quarter. The MPI software is required to run the fully optimized and parallelized version of RAMS. Once RAMS and MPI are completely installed on the AMU HP workstation, then sensitivity tests will be conducted to determine the likely cause(s) of the low-level cool bias in the version of RAMS used in ERDAS.

2.4   AMU CHIEF'S TECHNICAL ACTIVITIES (DR. MERCERET)

In July, Dr. Merceret presented a paper via teleconference to the 5th Annual Local Weather Technical Interchange Meeting (LW-TIM). The meeting was held 18-19 July and was hosted by the SMG at Johnson Space Center in Houston, TX. His paper was titled "The Lifetime of Mid-Tropospheric Wind Features as a Function of Their Vertical Scale".

In August and September, Dr. Merceret assisted in the analysis of field acoustic data and the design of a prototype demonstration experiment of the Hyper-SODAR at proposed SLF sites. This work is necessary to determine the feasibility of the sites as permanent Hyper-SODAR locations. Dr. Merceret also presented a paper describing the Lightning Launch Commit Criteria (Airborne Field Mill) Project at the American Meteorological Society (AMS) 9th Conference on Aviation, Range, and Aerospace Meteorology in Orlando, FL.

2.5   *TASK 001 AMU OPERATIONS*

Dr. Short, Ms. Lambert, and Mr. Case attended the LW-TIM at SMG. Dr. Short presented results from Phase I of the SIGMET IRIS task, Ms. Lambert presented results from Phase I of the Improved Anvil Forecasting task, and Mr. Case presented results from the ERDAS RAMS evaluation task.

Dr. Manobianco, Ms. Lambert, Mr. Case, and Dr. Short attended the AMS 9th Conference on Aviation, Range, and Aerospace Meteorology in Orlando, FL. Dr. Short and Mr. Case gave presentations of their AMU task results, and Dr. Manobianco and Ms. Lambert attended specific sessions with presentations relevant to current task work.

Mr. Wheeler finalized the purchase order for a hardware upgrade to an AMU IBM RS6000/260 system and coordinated the return and replacement of a tape backup unit. Ms. Lambert gathered images and text that could be used on the AMU Storyboard. A draft version of the text and images were sent to the graphic artists at ENSCO, Inc. for assimilation into a storyboard format.

NOTICE

Mention of a copyrighted, trademarked, or proprietary product, service, or document does not constitute endorsement thereof by the author, ENSCO, Inc., the AMU, the National Aeronautics and Space Administration, or the United States Government. Any such mention is solely for the purpose of fully informing the reader of the resources used to conduct the work reported herein.

List of Acronyms

30 SW	30th Space Wing
30 WS	30th Weather Squadron
45 LG	45th Logistics Group
45 OG	45th Operations Group
45 SE	45th Range Safety
45 SW	45th Space Wing
45 WS	45th Weather Squadron
AFB	Air Force Base
AFRL	Air Force Research Laboratory
AFSPC	Air Force Space Command
AFWA	Air Force Weather Agency
AMS	American Meteorological Society
AMU	Applied Meteorology Unit
AP	Anomalous Propagation
AWIPS	Advanced Weather Interactive Processing System
CAR	Core Aspect Ratio
CCAFS	Cape Canaveral Air Force Station
CGLSS	Cloud to Ground Lightning Surveillance System
COF	PAFB 3-Letter Identifier
CSI	Critical Success Index
CSR	Computer Sciences Raytheon
CVIL	Cell-based VIL
DOD EAFC	Department of Defense Eastern Area Frequency Coordinator
EDA	Exploratory Data Analysis
EOM	End of Mission
ERDAS	Eastern Range Dispersion Assessment System
FAR	False Alarm Rate
FR	Shuttle Flight Rules
FSL	Forecast Systems Laboratory
FSU	Florida State University
FY	Fiscal Year
GNV	Gainesville, FL 3-Letter Identifier
GOES	Geostationary Operational Environmental Satellite
HMAX	Height of Maximum Reflectivity
HP	Hewlett Packard
HSS	Heidke Skill Score
HYPACT	Hybrid Particle and Concentration Transport
I&M	Improvement and Modernization
IRIS	SIGMET's Integrated Radar Information System
JAX	Jacksonville, FL 3-Letter Identifier
JSC	Johnson Space Center

List of Acronyms

KSC	Kennedy Space Center
LAPS	Local Analysis and Prediction System
LCC	Launch Commit Criteria
LDIS	Local Data Integration System
LW-TIM	Local Weather Technical Interchange Meeting
MAX	Maximum Reflectivity
MIDDS	Meteorological Interactive Data Display System
MHz	Mega-Hertz
MLB	Melbourne, FL 3-Letter Identifier
MPI	Message Passing Interface
MSFC	Marshall Space Flight Center
NASA	National Aeronautics and Space Administration
NCAR	National Center for Atmospheric Research
NE	Northeast
NOAA	National Oceanic and Atmospheric Administration
NPA	Pensacola, FL 3-Letter Identifier
NSSL	National Severe Storms Laboratory
NWP	Numerical Weather Prediction
NWS MLB	National Weather Service in Melbourne, FL
PAFB	Patrick Air Force Base
POD	Probability of Detection
PUP	Principle User Processor
RAMS	Regional Atmospheric Modeling System
REEDM	Rocket Exhaust Effluent Dispersion Model
RIDDS	Radar Interface and Data Distribution System
RMS	Root Mean Square
RSA	Range Standardization and Automation
RTLS	Return to Launch Site
RUC	Rapid Update Cycle NWP Model
SE US	Southeast United States
SIL	Slidell, LA 3-Letter Identifier
SLF	Shuttle Landing Facility
SMC	Space and Missile Center
SMG	Spaceflight Meteorology Group
ST	Storm Top
STS	Shuttle Transportation System
TBW	Ruskin, FL 3-Letter Identifier
TLH	Tallahassee, FL 3-Letter Identifier
TTS	SLF 3-Letter Identifier
USAF	United States Air Force
UTC	Universal Coordinated Time
VIL	Vertically Integrated Liquid

List of Acronyms

W	West
WGP	Wind Gust Potential
WSR-74C	Weather Surveillance Radar, model 74C
WSR-88D	Weather Surveillance Radar 1988 Doppler
WWW	World Wide Web
XMR	CCAFS 3-Letter Identifier

AMU Project Schedule				
31 October 2000				
AMU Projects	Milestones	Actual / Projected Begin Date	Actual / Projected End Date	Notes/Status
Statistical Forecast Guidance (Ceilings)	Determine Predictand(s)	Aug 98	Sep 98	Completed
	Data Collection, Formulation and Method Selection	Sep 98	Apr 99	Completed
	Equation Development, Tests with Independent Data, and Tests with Individual Cases	Apr 00	Nov 00	On Schedule
	Prepare Products, Final Report for Distribution	Nov 00	Feb 01	On Schedule
Statistical Forecast Guidance (Winds)	Determine Predictand(s)	Feb 01	Mar 01	On Schedule
	Data Reduction, Formulation and Method Selection	Mar 01	May 01	On Schedule
	Equation Development, Tests with Independent Data, and Tests with Individual Cases	May 01	Sep 01	On Schedule
	Prepare Products, Final Report for Distribution	Sep 01	Dec 01	On Schedule
Meso-Model Evaluation	Develop ERDAS RAMS Evaluation Protocol	Feb 99	Mar 99	Completed
	Perform ERDAS RAMS Evaluation	Apr 99	Sep 99	Completed
	Extend ERDAS RAMS Evaluation	Oct 99	Oct 00	Processing Data for Analysis
	Interim ERDAS RAMS Report	Dec 99	Aug 00	Completed
	Final ERDAS RAMS Report	Oct 00	Dec 00	On Schedule
Delta Explosion Analysis	Analyze Radar Imagery	Jun 97	Nov 97	Completed
	Run Models/Analyze Results	Jun 97	Jun 98	Completed
	Final Report	Feb 98	Sep 00	Completed
	Launch Site Climatology Plan	Apr 98	May 98	Completed
Detecting Chaff Source Regions	Detect and analyze chaff signatures for source region	Oct 99	Apr 00	Completed
	Final Report	Apr 00	Aug 00	Competed
Extended Evaluation of CAR	Evaluate predictive capabilities for wind gust and hail events	Jul 00	Sep 00	Completed
	Final Report	Sep 00	Oct 00	Internal Review
SIGMET IRIS Processor Evaluation Phase II	Develop and transition new products to 45 WS IRIS station	Apr 00	Apr 01	On Schedule
	Final Report	May 01	Jun 01	On Schedule

AMU Project Schedule 31 October 2000				
AMU Projects	Milestones	Actual / Projected Begin Date	Actual / Projected End Date	Notes/Status
LDIS Extension: Phase III	Assistance in installation at NWS MLB	Jan 00	Oct 00	Delayed – waiting for setup of data connections
	Assistance in installation at SMG	Apr 00	Jul 00	Completed
	Memorandum describing LDIS transition to real-time operations	Jul 00	Oct 00	Delayed to complete installation at SMG and NWS MLB
	Technical collaboration with SMG towards a conference paper	Aug 00	Oct 00	Delayed
ERDAS RAMS Extension Task	Memorandum summarizing data transfer feasibility to SMG & NWS MLB	Jul 00	Oct 00	Delayed – developing code to test data transfer
	Enhancement of verification Graphical User Interface	Apr 00	Feb 01	On Schedule
	Implement data transfer	Sep 00	Nov 00	On Schedule
	Input of methodology and results into ERDAS RAMS final report	Nov 00	Dec 00	On Schedule